New Current Sheet and Magnetic Field Models of the Jovian Magnetosphere for Pre-Galileo, Galileo and Juno Era

Naoya Momoki[1] and Hiroaki Toh[2]

[1]Division of Earth and Planetary Sciences, Graduate School of Science, Kyoto University
[2]Graduate School of Science, Kyoto University

November 26, 2022

Abstract

In the Jovian magnetosphere, an electric current system within the 'current sheet' generates a magnetic field, which is comparable to or dominating the Jovian intrinsic field in the nightside magnetosphere. However, update of an existing model of the magnetospheric field using newly acquired data by Galileo and Juno have never been conducted since it was first formulated in 1997. Here we used the data by Voyager 1/2, Galileo and Juno to revise the current sheet model as well as the magnetospheric field model based on each spacecraft data. We derived models that reproduced each data well, and revealed long-term variations of both current sheet and magnetospheric field over several decades. The updated models were found useful to detect dynamic events in the magnetosphere such as magnetopause deformation and plasmoid generation. They can also be used as external fields necessary for probing into the Galilean icy moons by electromagnetic induction methods.

Hosted file

`supporting_information.docx` available at https://authorea.com/users/539778/articles/605632-new-current-sheet-and-magnetic-field-models-of-the-jovian-magnetosphere-for-pre-galileo-galileo-and-juno-era

Hosted file

`essoar.10508693.1.docx` available at https://authorea.com/users/539778/articles/605632-new-current-sheet-and-magnetic-field-models-of-the-jovian-magnetosphere-for-pre-galileo-galileo-and-juno-era

Naoya Momoki[1] and Hiroaki Toh[2]

[1] Division of Earth and Planetary Sciences, Graduate School of Science, Kyoto University

[2] Data Analysis Center for Geomagnetism and Space Magnetism, Graduate School of Science, Kyoto University

Corresponding author: Naoya Momoki (momoki@kugi.kyoto-u.ac.jp)

Key Points:

- We updated existing models of both current sheet and magnetic field in the Jovian magnetosphere using pre-Galileo, Galileo and Juno data.
- Differences among the updated models may represent decadal variations of the current system in the Jovian magnetosphere.
- The models are useful for study on magnetospheric dynamics and prediction of temporal magnetic variations external to Galilean icy moons.

Abstract

In the Jovian magnetosphere, an electric current system within the 'current sheet' generates a magnetic field, which is comparable to or dominating the Jovian intrinsic field in the nightside magnetosphere. However, update of an existing model of the magnetospheric field using newly acquired data by Galileo and Juno have never been conducted since it was first formulated in 1997. Here we used the data by Voyager 1/2, Galileo and Juno to revise the current sheet model as well as the magnetospheric field model based on each spacecraft data. We derived models that reproduced each data well, and revealed long-term variations of both current sheet and magnetospheric field over several decades. The updated models were found useful to detect dynamic events in the magnetosphere such as magnetopause deformation and plasmoid generation. They can also be used as external fields necessary for probing into the Galilean icy moons by electromagnetic induction methods.

Plain Language Summary

Above Jupiter's atmosphere and ionosphere, there is a vast region coined 'magnetosphere' where magnetic fields govern physical phenomena. The magnetic fields in the magnetosphere are divided mainly into two components: one arising from inside Jupiter, and the other generated by electric currents flowing in a current sheet in the nightside magnetosphere. Although both had been modeled so far, the models are, as usual, not perfect and should be updated on arrival of new datasets. Unfortunately, one of the models of the magnetospheric field is especially far from up to date, compared with the intrinsic field. In this study, we focused on the magnetospheric field and its associated current sheet models using three datasets by four spacecraft, pre-Galileo (Voyager 1 and Voyager 2), Galileo and Juno. By updating the models for each dataset, we determined three pairs of current sheet and magnetospheric field that showed long-term

variations of Jupiter's magnetosphere over nearly half a century. The three pairs are also found useful to detect dynamic events in the Jovian magnetosphere such as temporal changes of its shape and coherent plasma releases, and for probing deep into the Galilean icy moons that are thought to be possible cradles of extraterrestrial lives.

1 Introduction

The Jovian magnetosphere has been probed by several spacecraft and thus vector magnetic data have also been accumulated intermittently. Since the first flyby to Jupiter by Pioneer 10 in 1973, five spacecraft (Pioneer 11, Voyager 1, Voyager 2, Ulysses and Cassini) flew by and conducted magnetic observations. Galileo was the very first orbiter inserted into Jovicentric orbits, and now Juno is in Jupiter's polar orbits. One of the main applications of the magnetic data is modeling of the Jovian magnetic field which mainly consists of the Jovian intrinsic and magnetospheric magnetic fields.

The Jovian intrinsic field is originated from the dynamo action inside Jupiter. Its models have been studied intensively since the first observation by Pioneer 10, e.g., Smith et al. (1974), O_6 (Connerney, 1992), VIP4 (Connerney et al., 1998), VIT4 (Connerney, 2007), VIPAL (Hess et al., 2011), Ridley and Holme (2016) and JRM09 (Connerney et al., 2018). The models are described by a scalar potential that is a series expansion of spherical harmonics, and have been improved whenever new and better data were delivered. On the other hand, the magnetospheric field is originated from electric current systems outside Jupiter such as current sheet and magnetopause currents, and its models have been studied by fewer reseachers (e.g., Alexeev & Belenkaya, 2005; Connerney et al., 1981; Khurana, 1997). Updates of the models using new data by Galileo and/or Juno are limited (e.g., Connerney et al., 2020) and have not caught up with the accumulation of the data. Nevertheless, the magnetospheric field models have a wide range of applications such as predicting the magnetic field that a spacecraft may observe (e.g. Kivelson et al., 1997), calculating the magnetic field external to Jupiter's satellites for electromagnetic (EM) induction studies (e.g. Khurana et al., 2009) and so on.

We adopted the combined formulation of the magnetospheric field by Khurana (1997) and the shape of the current sheet by Khurana (1992) in this study. First, we updated the current sheet shape model parameters for each dataset by Galileo and Juno in addition to the pre-Galileo spacecraft (Voyager 1 and 2) as described in the next section. We then redetermined Euler potentials (Stern, 1970, 1976) of the magnetospheric field to investigate the possible long-term variation of the current sheet and the magnetospheric field by comparing the three sets of updated models. The newly updated models have a wide range of application such as detecting magnetospheric dynamic phenomena associated with magnetotail reconnections and magnetopause variations. They are also capable of prediction of inducing fields at each Galilean icy moon for EM induction purposes. The new models are of use for the future missions, JUICE and Europa Clipper, as well in order to know the magnetospheric field along their

trajectories.

2 Models

Khurana's (1997) model that we adopted in this study is an Euler potential model of the magnetic field generated by electric currents flowing within the current sheet on the nightside magnetosphere. The shape of the current sheet varies with Jupiter's rotation and is influenced by the shape of the magnetosphere (Khurana & Kivelson, 1989; Northrop et al., 1974). It is also necessary to model it as a function of time, or local time before deriving the Euler potentials as had been done by Khurana (1992).

$$\begin{aligned} Z_{\mathrm{CS}} &= \rho \tan(\theta_d) \frac{x_0}{x} \tanh\left(\frac{x}{x_0}\right) \cos(\lambda - \delta) \\ \delta &= \lambda_d + \frac{\Omega_J \rho_0}{v_0} \ln\cosh\left(\frac{\rho}{\rho_0}\right) \end{aligned} \quad \#(\ SEQ\ Equation\ \backslash *\ ARABIC\ 1)$$

The current sheet model adopted here is characterized by the following three parameters: (x_0, ρ_0, v_0). An advantage of Khurana's (1992) model is that it can replicate two features of the current sheet that were revealed by past observations, namely, bendback and hinge. The bendback is an axisymmetric effect that the current sheet distorts westward with the increasing ρ, and manifests in δ. It is caused by the finite propagation velocity of the tilted magnetic dipole oscillation associated with Jupiter's rotations and/or the non-corotating plasmas in the middle and the outer magnetosphere (Khurana, 1997; Northrop et al., 1974). On the other hand, the hinge is a non-axisymmetric effect that the Z_{CS} is saturated by the solar wind, and thus a strong function of x. While the bendback results in delayed encounters of a spacecraft with the current sheet (Northrop et al., 1974), the hinge promotes earlier encounters in some cases. When a spacecraft is located in the north of the Jovigraphic equator, the hinged current sheet results in delayed encounters when the spacecraft crosses the current sheet from north to south. However, earlier encounters occur at the time of south to north crossings (Bridge et al., 1979; Ness et al., 1979).

$$\begin{aligned} \mathbf{B} &= f \times g \\ f &= -C_1 \rho_m \left[\tanh\left(\frac{r_{01}}{r}\right)\right]^{a_1} \ln\cosh\left(\frac{Z_m - Z_{m,CS}}{D_1}\right) \\ &\quad + \int \rho_m \left\{C_2 \left[\tanh\left(\frac{\rho_{02}}{\rho_m}\right)\right]^{a_2} + C_3 \left[\tanh\left(\frac{\rho_{03}}{\rho_m}\right)\right]^{a_3} + C_4\right\} d\rho_m \\ g &= \phi + p\left[1 + q\ \tanh^2\left(\frac{Z_m - Z_{m,CS}}{D_2}\right)\right] \rho_m \end{aligned} \quad \#(\ SEQ\ Equation\ \backslash *\ ARABIC$$

In the previous studies, the data by Pioneer 10, Voyager 1 and Voyager 2 were used to determine the seventeen parameters above. When constructing these models, a Jovian intrinsic field model was necessary. While O_6 model was adopted in the previous studies, in this study we adopted the latest JRM09 model determined using the Juno data . Although the secular variations of the intrinsic field may present (Moore et al, 2019; Ridley & Holme, 2016; Yu et al,

2010), we applied the model to all the spacecraft data. This means that we neglected the secular variation of the intrinsic field.

3 Data

In this study, we used the magnetic field data by Voyager 1/2, Galileo and Juno available at NASA's Planetary Data System. As for Juno, data from the initial 23 orbits and the first half of the 24th orbit were used. Following the previous studies, we adopted the data at Jovicentric distances from 10 to 100 R_J ($1R_J$=71,492km) and in the nightside (from 1800 to 0600 LT).

We updated the models by optimizing their parameters using the new data. For the current sheet model, we extracted the estimated positions of the spacecraft's current sheet crossing from the magnetic data. Because the range of possible crossing latitudes are nearly equal to that of dipole equator latitudes, we restricted the latitude of the data in addition to the constraints on the Jovicentric distance and the local time. Specifically, we adopted the data within the Jovicentric latitudes of $\pm 10.31^\circ$ corresponding to the θ_d of the JRM09 model.

We can find the current sheet crossings by zero radial components of the magnetic field data. To pick up the crossings, we first took 60 minutes running averages of the data and identified the zero radial components in the smoothed data as candidates for the crossings. Then, we selected a final set of the crossings by imposing two constraints on the candidates: (1) cadense of the crossings and (2) coincidence with minima of the magnetic field strength data. The non-zero θ_d results in the oscillation of the current sheet from the Jovigraphic equator caused by Jupiter's rotation. This means that two crossings per rotation are expected to occur at relatively low latitudes associated with the periodic movement of the current sheet. Taking advantage of this scenario, we excluded non-periodic candidates (e.g., multiple crossings in a short time). Since we can reasonably assume that in the steady state, the pressure in the current sheet balances that in the lobe (Lanzerotti et al., 1980), we can expect that minima of the magnetic field strength coincide with the crossings. Using this rule of thumb, we excluded candidates that lose clear correlation with the field strength. Thanks to the two constraints introduced here, we succeeded in extracting reliable current sheet crossings for use in the subsequent model updates.

For the magnetospheric field model, we consider the observed vector magnetic data as a sum of the Jovian intrinsic and magnetospheric field. In addition, magnetospheric fields by current systems except for that in the current sheet itself are assumed small enough within the region of the magnetosphere of this study. Under these assumptions, we defined the observed magnetospheric field as vector deviations from the intrinsic field model (JRM09).

4 Methods

Following the previous studies, we updated the models in two steps. First, we determined the three parameters of the current sheet model based on Khurana (1992), and second, we estimated the fourteen parameters of the magnetospheric

field model based on Khurana (1997) by fixing the current sheet parameters as known constants, instead of determining all the paramters simultaneously. We reorganized the magnetic data by four spacecraft into three datasets, pre-Galileo (Voyager 1 and 2), Galileo and Juno, and updated the models for each dataset. In other words, we determined three pairs of shape and field models so that we may find long-term variations of the current sheet or the field, if any, by comparing the three.

As a method of optimization, we adopted a least square method with a gradient search technique. It searches for a parameter set by minimizing the root mean squared differences between the model and the data in the parameter space. While the technique can find a local minimum, it is not guaranteed that the detected minimum is the global minimum. To circumvent the difficulty, the technique is usually implemented with a considerable number of initial parameter sets. We optimized the parameters from 125 initial sets for the current sheet model and 100 initial sets for the magnetospheric field model.

$$\lambda_{\rm model} \quad = \quad \delta_{\rm data} \pm \cos^{-1}\left\{ Z_{CS,data}\left[\rho_{\rm data}\tan\left(\theta_d\right)\frac{x_0}{x_{\rm data}}\tanh\left(\frac{x_{\rm data}}{x_0}\right)\right]^{-1}\right\}, \#(\ SEQ\ Equation\ \backslash *\ ARABIC\ 4)$$

For calculating the root mean squared differences necessary for the magnetospheric field model, we used all the three components of the modeled and the observed magnetic field.

5 Results

The current sheet crossings detected by the method mentioned in the previous section are shown in Figure 1. The numbers of the crossings are 45 for pre-Galileo, 2283 for Galileo and 657 for Juno, which are mainly depend on each spacecraft's trajectory. The updated model parameters of the current sheet are listed in Table 1 together with RMSs in addition to those of Khurana (1992). Although we updated them with the method different from that of Khurana (1992), the determined parameters of the pre-Galileo model (especially x_0 and v_0 that are not affected significantly by the choice of the intrinsic model) are consistent with those of Khurana (1992) model, which means validity of using the west longitudes for updates. An example of the comparison between the detected crossings and the modeled current sheet is shown in Figure 2a. The detected crossings show two features: (1) the westward shift with the increasing ρ by the bendback and (2) the proximity to δ or $\delta + 180^\circ$ by the hinge and/or spacecraft's migration into high latitudes, and the model reproduces these well. Although it is the average model using all the data from the full mission period each, the figure indicates that it is useful for the prediction

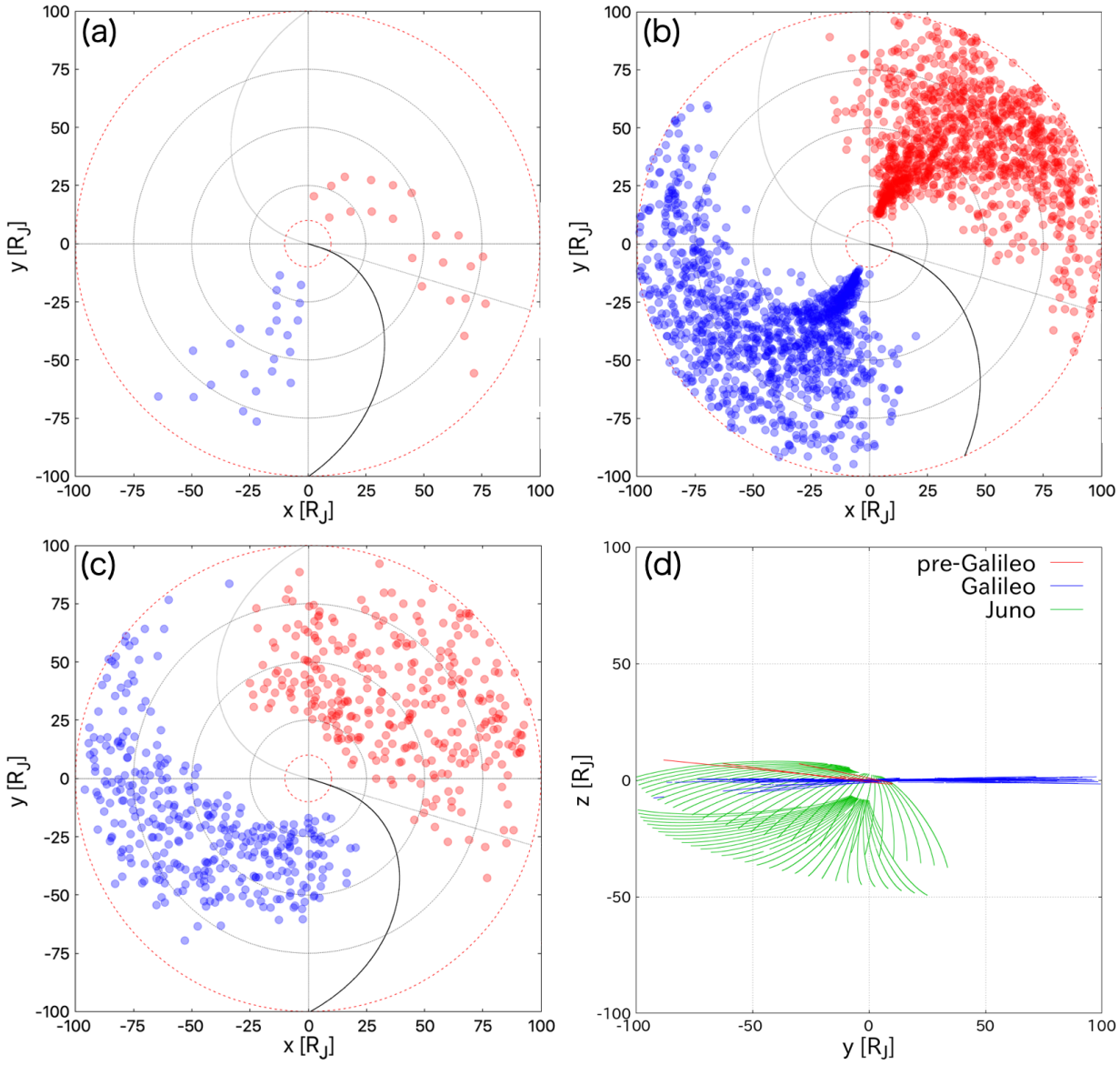

Fig 1. (a)–(c) Distribution of the crossings observed by Voyager 1/2, Galileo and Juno, respectively, projected on the Jovigraphical equatorial plane with the System III prime meridian as x-axis. x and y coordinates are measured in units of R_J. Red circles represent north-to-south crossings of the current sheet while blue ones correspond to south-to-north crossings. Red dashed circles represent the distance range of the used data (10 R_J and 100 R_J, respectively). Black and gray curves denote δ and $\delta + 180^\circ$ as functions of the $\rho = \sqrt{x^2 + y^2}$. 45 crossings observed by Voyager 1/2, 2283 by Galileo and 657 by Juno. (d)

Trajectories of each spacecraft within the same distance range, projected on the y-z plane of the Jupiter de-Spun Sun coordinate system. Both coordinates are measured in units of R_J. Red, blue and green lines represent the trajectories of Voyager 1/2, Galileo and Juno, respectively.

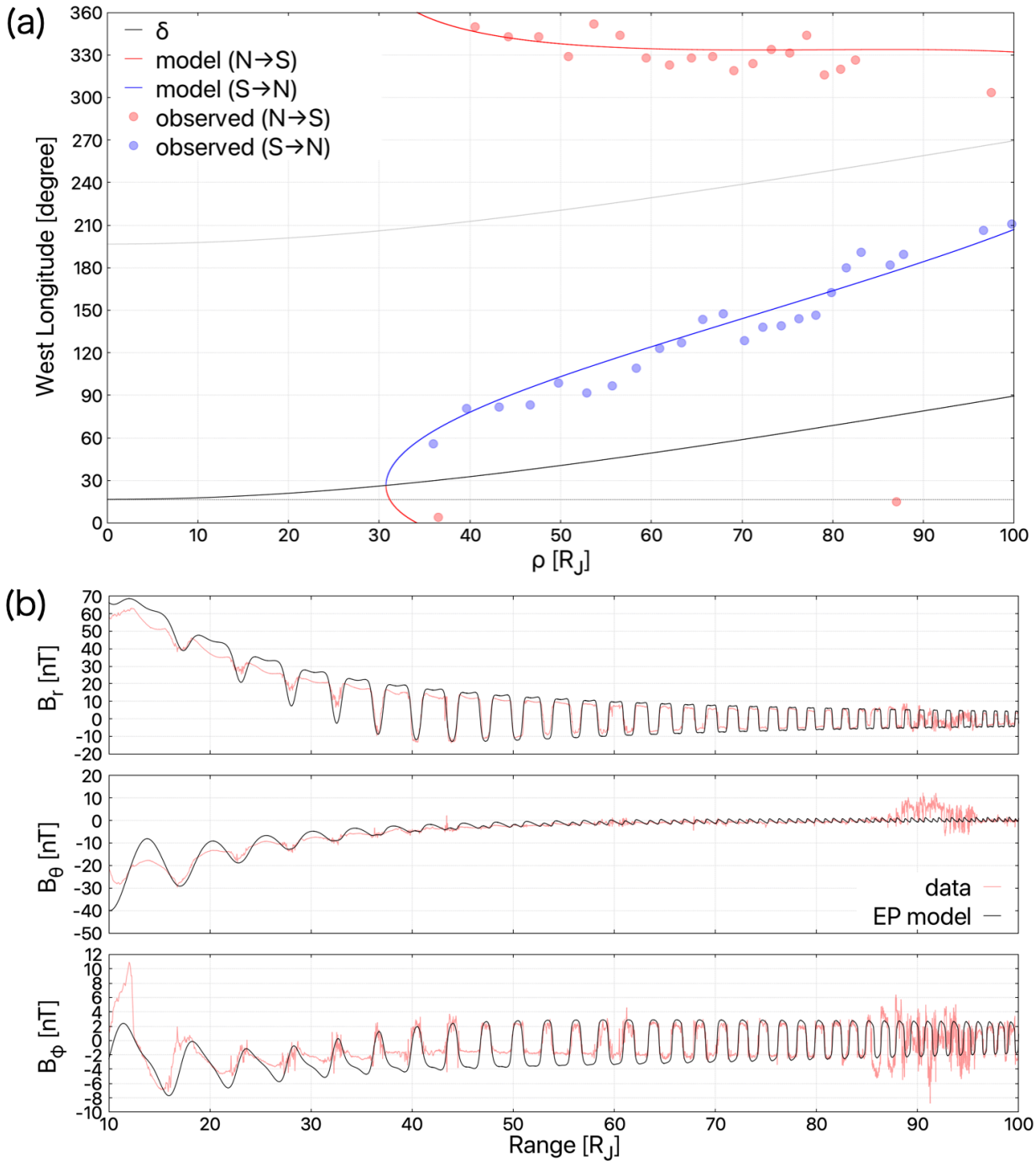

Figure 2. Comparison of the model predictions and the data on the inbound trajectory of the Juno peri-06. (a) The current sheet crossing data (circles)

and the updated current sheet (lines) in System III coordinates for 10 $R_J < \rho < 100$ R_J. The red circles and line indicate the north-to-south crossings, while the south-to-north results are shown in blue. Black and gray curves represent δ and $\delta + 180^\circ$ as in Fig. 1. (b) The magnetospheric field (observation minus JRM09) by Juno (red) and the modeled field (black) in System III coordinates for 10 $R_J < r < 100$ R_J. The top, middle and bottom panels show B_r, B_θ and B_ϕ in nT, respectively.

of the crossings at each orbit.

The updated model parameters of the magnetospheric field and RMSs are also listed in Table 1 together with those of Khurana's (1997) common model. Comparison of the magnetospheric magnetic data with the model predictions is shown in Figure 2b. B_r and B_ϕ show periodic variations associated with Jupiter's rotation and B_θ represents a northward magnetic field by eastward electric currents within the current sheet. The updated model fits the observed data well except for a fluctuation seen at around 90 R_J, which implies a possible detection of a dynamic event in the pre-dawn magnetosphere. We will argue the implication of this in the next section.

6 Discussion

Differences of the bendback effect among the updated current sheet models can be estimated by v_0 values listed in Table 1 and Figure S1 showing the δ curves of each model in the

Table 1. The updated model paramters and their RMSs by pre-Galileo, Galileo and Juno together with those by Khurana (1992, 1997) for both current sheet and magnetospheric field. The parameters of Khurana (1997) are those of the common model.

Current sheet	pre-Galileo	Galileo	Juno	Khurana (1992)
x_0	-36.1	-35.2	-43.5	33.5
ρ_0	14.9	29.2	49.9	33.2
v_0	44.5	58.9	33.0	37.4
RMS [degree]	10.5	22.0	19.1	11.2
Magnetic field	pre-Galileo	Galileo	Juno	Khurana (1997)
C_1	95.3	112.2	177.2	80.3
C_2	1852.5	874.6	61.1	690.4
C_3	-228.3	40.5	78.7	101.3
C_4	-1.4	-0.81	-0.79	-1.7
a_1	2.19	2.28	1.71	2.49
a_2	2.20	2.80	286.51	1.80
a_3	20.50	4.68	2.83	2.64
r_{01}	34.6	28.9	20.3	38.0
ρ_{02}	3.13	4.07	18.99	2.14
ρ_{03}	16.9	25.5	16.9	12.5
D_1	2.30	2.36	2.66	2.01

Current sheet	pre-Galileo	Galileo	Juno	Khurana (1992)
D_2	14.60	9.69	18.19	13.27
p	4.53	3.79	3.94	6.26
q	0.77	0.32	0.58	0.35
RMS [nT]	3.778	3.950	2.859	4.01

Jovigraphic equatorial plane. The v_0 values whose reciprocals determine the bendback strength and the curves indicate a weak bendback of the Galileo model. Because the v_0 corresponds to the Alfvén velocity that conveys Jupiter's rotation phase to the current sheet, the weak bendback of the Galileo model implies a relatively large Alfvén velocity during the Galileo era. Although it is still an open question what created the different Alfvén velocities, the long-term variation over several decades was found for the first time by this study. One concern is the difference in spacecraft's trajectories as well as the reported spatial dependence of the bendback (Khurana, 2001; Khurana & Schwarzl, 2005). We must be careful in distinguishing the detected changes from the spatial dependence of the current sheet in order to interpret it in terms of temporal variations.

The comparative study on $|x_0|$ values listed in Table 1 may reveal temporal variations of the hinge effect, which is also shown in Figure S2 in the form of cross-sections of the current sheets in either the midnight meridian or the pseudo prime meridian ($\lambda = \delta$) at midnight. The relatively large $|x_0|$ value and the maximum Z_{CS} of the cross-section indicates the weak hinge of the Juno model. Although the hinge can be strengthened by the compression of the magnetosphere with increasing solar wind dynamic pressure, it is difficult to know the actual solar wind parameters near Jupiter when a spacecraft is in the magnetosphere. One of the indices that correlates with the averaged dynamic pressure is the solar activity that manifests in the sunspot numbers (Jackman & Arridge, 2011). The solar activity is minimum in the Juno era, while it was close to maximum in both Voyager and Galileo eras. If the averaged dynamic pressure is weaker in the period of the minimum solar activity, it may explain the large maximum Z_{CS} found in this study. The long-term variation of Z_{CS} has not been reported before and may imply that the influence of the solar wind can reach the low-latitude magnetosphere that has been thought 'rotation driven' so far. The short-period change of the hinge is also seen in the Figure 2a and its investigation is useful for estimating the changes of the solar wind parameters or the shape of the magnetosphere, though they are beyond the scope of this study.

Magnetospheric magnetic data sometimes include irregular fluctuations. An example

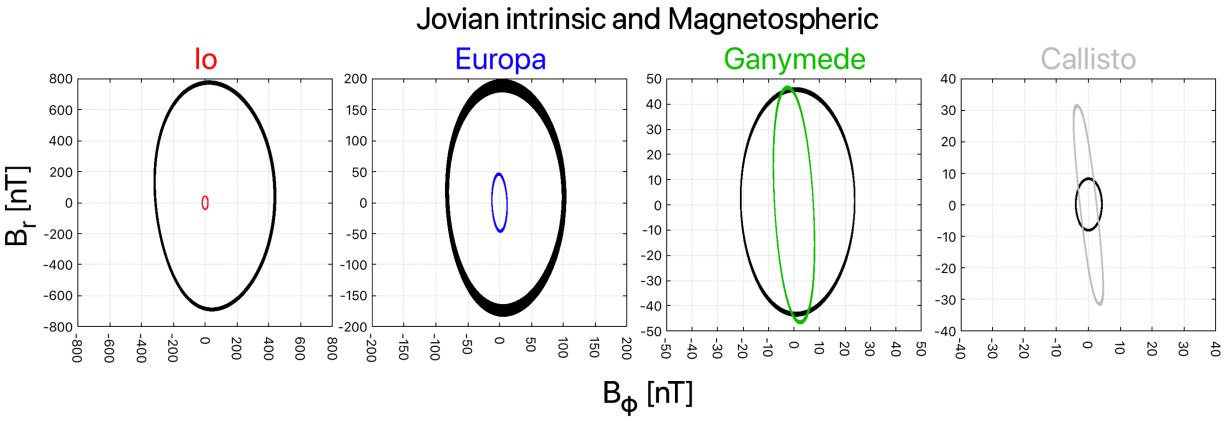

Figure 3. Hodograms of B_r and B_ϕ components of the intrinsic field (JRM09, black) and the updated magnetospheric field by Juno (other colors) at each Galilean satellite in nT. The variations associated with Jupiter's rotation manifest in elliptical trajectories of the magnetic field, while those of each satellite's revolution appear in thickness of the trajectories.

observed in Juno's peri-06 has already been shown in the Figure 2b near 90 R_J. These fluctuations are significant especially in the outer magnetosphere with smaller frequencies than that of the Jovian rotation. It, therefore, is natural to consider them being caused by magnetic reconnections in the magnetotail or spacecraft's magnetopause crossings. Although these events in the Juno era have been reported (e.g., Gershman et al., 2017; Hospodarsky et al., 2017; Vogt et al., 2020), their researches were confined to a few initial orbits. In this study, we did not remove the fluctuations explicitly from the magnetic data and the updated models are possibly biased by them. The fluctuations associated with the reconnections and/or the magnetopause can be defined by deviations from the updated magnetospheric field models. One of the future works of this study is detection and removal of them using the updated models as the first order approximation. The detection of the events leads to further understanding of the magnetospheric dynamics, and the removal of them will result in reconstruction of both current sheet and magnetospheric field models with more precision.

Among Jupiter's satellites, Europa, Ganymede and Callisto are covered with ice and possible presence of subsurface oceans has been argued (Jia et al., 2010). One of the major methods to investigate them is the EM induction method. The electrical structure of the icy moons can be estimated by subtracting the predicted external field (magnetospheric plus intrinsic) from the data and taking ratios of the induced to the external fields. Figure 3 shows hodograms of the magnetic field around each Galilean satellite using JRM09 and the magnetospheric field of the Juno era. Each satellite feels periodic magnetic variations caused by Jupiter's rotation and satellite's revolution. Figure 3 indicates that the Jovian intrinsic field is dominant at Io and Europa because of their proximity

to Jupiter, while the magnetospheric field is dominant at Callisto, the farthest Galilean satellite from Jupiter, and comparable at Ganymede. The magnetospheric field, therefore, also plays an important role in the subsurface ocean investigations by the EM induction method. In the near future, two spacecraft missions, JUICE targeting Ganymede and Europa Clipper targeting Europa, will be carried out. It is expected that long-term continuous magnetic field data on satellite-centric orbits will be provided, whose interpretation in terms of the EM induction method can be conducted with the help of the updated models of this study.

7 Summary

In this study, we started with updating the current sheet shape by following Khurana (1992). The new data by Galileo and Juno in addition to the data by Voyager 1/2 were used. The three derived models (pre-Galileo, Galileo and Juno) can deal with two features of the current sheet, i.e., bendback and hinge. We found out the weak bendback in the Galileo model and the weak hinge in the Juno model. The former can be interpreted as a signature of increased Alfvén velocity in the magnetosphere. Although further investigations on both plasma and orbital effects (e.g., an analysis using spatially binned data) are necessary, the result may imply that there are decadal variations of the magnetic field as well as the plasma environment in the magnetosphere. The latter can be attributed to the weak dynamic pressure of the solar wind in the Juno era. Although it is not clear whether the relatively low current sheet heights of the other models are biased by spacecraft's trajectories, it may be a good example showing the close coupling between the solar wind and the Jovian magnetosphere.

We also updated the magnetospheric field model by following Khurana (1997). The derived models fit the data well and the fluctuations by magnetic reconnections or magnetopause crossings were found in the data as the deviations from the updated models. Detections of those deviations using the updated models are important to understand the dynamics of the Jovian magnetosphere and to re-update the models with more precision. Being combined with the Jovian intrinsic field model, the magnetospheric field models can be used to predict temporal variations of the magnetic field at each Galilean satellite for EM induction studies. New spacecraft missions, JUICE and Europa Clipper, are planned and the models updated by this study will be of use for the future investigations by new probes.

Acknowledgments, Samples, and Data

The magnetic field data of Voyager 1 (https://pds-ppi.igpp.ucla.edu/search/view/?f=yes&id=pds://PPI/vg1-mag-jup/data-s3coords-48sec), Voyager 2 (https://pds-ppi.igpp.ucla.edu/search/view?f=yes&id=pds://PPI/VJ-MAG-4-SUMM-S3COORDS-48.0SEC-V1.1), Galileo (https://pds-ppi.igpp.ucla.edu/search/view?f=yes&id=J-MAG-3-RDR-MAGSPHERIC-SURVEY-V1.0) and Juno (https://pds-ppi.igpp.ucla.edu/data/JNO-J-3-FGM-CAL-V1.0/) are available from NASA's Planetary Data System.

References

Alexeev, I. I., & Belenkaya, E. S. (2005). Modeling of the Jovian magnetosphere. *Annales Geophysicae*, *23*(3), 809–826. https://doi.org/10.5194/angeo-23-809-2005

Bridge, H. S., Belcher, J. W., Lazarus, A. J., Sullivan, J. D., McNutt, R. L., Bagenal, F., et al. (1979). Plasma observations near Jupiter: Initial results from Voyager 1. *Science*, *204*(4396), 987–991. https://doi.org/10.1126/science.204.4396.987

Connerney, J. E. P. (1992). Doing more with Jupiter's magnetic field. In H. O. Rucker, S. J. Bauer, & M. L. Kaiser (Eds.), *Planetary radio emissions III* (pp. 13–33). Vienna: Austrian Academy of Sciences Press.

Connerney, J. E. P. (2007). Planetary magnetism. In G. Schubert (Eds.), *Treatise on geophysics* (Vol. 10, pp. 243–280). Oxford: Elsevier.

Connerney, J. E. P., Acuña, M. H., & Ness, N. F. (1981). Modeling the Jovian current sheet and inner magnetosphere. *Journal of Geophysical Research: Space Physics*, *86*(A10), 8370–8384. https://doi.org/10.1029/JA086iA10p08370

Connerney, J. E. P., Acuña, M. H., Ness, N. F., & Satoh, T. (1998). New models of Jupiter's magnetic field constrained by the Io flux tube footprint. *Journal of Geophysical Research: Space Physics*, *103*(A6), 11,929–11,939. https://doi.org/10.1029/97JA03726

Connerney, J. E. P., Kotsiaros, S., Oliversen, R. J., Espley, J. R., Joergensen, J. L., Joergensen, P. S., et al. (2018). A new model of Jupiter's magnetic field from Juno's first nine orbits. *Geophysical Research Letters*, *45*(6), 2590–2596. https://doi.org/10.1002/2018GL077312

Connerney, J. E. P., Timmins, S., Herceg, M., & Joergensen, J. L. (2020). A Jovian magnetodisc model for the Juno era. *Journal of Geophysical Research: Space Physics*, *125*(10), e2020JA028138. https://doi.org/10.1029/2020JA028138

Gershman, D. J., DiBraccio, G. A., Connerney, J. E. P., Hospodarsky, G., Kurth, W. S., Ebert, R. W., et al. (2017). Juno observations of large-scale compressions of Jupiter's dawnside magnetopause. *Geophysical Research Letters*, *44*(15), 7559–7568. https://doi.org/10.1002/2017GL073132

Gurnett, D. A., Scarf, F. L., Kurth, W. S., Shaw, R. R., & Poynter, R. L. (1981). Determination of Jupiter's electron density profile from plasma wave observations. *Journal of Geophysical Research: Space Physics*, *86*(A10), 8199–8212. https://doi.org/10.1029/JA086iA10p08199

Hess, S. L. G., Bonfond, B., Zarka, P., & Grodent, D. (2011). Model of the Jovian magnetic field topology constrained by the Io auroral emissions. *Journal of Geophysical Research: Space Physics*, *116*(A5). https://doi.org/10.1029/2010JA016262

Hospodarsky, G. B., Kurth, W. S., Bolton, S. J., Allegrini, F., Clark, G. B., Connerney, J. E. P., et al. (2017). Jovian bow shock and magnetopause encounters by the Juno spacecraft. *Geophysical Research Letters*, *44*(10), 4506–4512. https://doi.org/10.1002/2017GL073177

Jackman, C. M., & Arridge, C. S. (2011). Solar cycle effects on the dynamics of Jupiter's and Saturn's magnetospheres. *Solar Physics*, *274*, 481–502. https://doi.org/10.1007/s11207-011-9748-z

Jia, X., Kivelson, M. G., Khurana, K. K., & Walker, R. J. (2010). Magnetic fields of the satellites of Jupiter and Saturn. *Space Science Reviews*, *152*, 271–305. https://doi.org/10.1007/s11214-009-9507-8

Khurana, K. K. (1992). A generalized hinged-magnetodisc model of Jupiter's nightside current sheet. *Journal of Geophysical Research: Space Physics*, *97*(A5), 6269–6276. https://doi.org/10.1029/92JA00169

Khurana, K. K. (1997). Euler potential models of Jupiter's magnetospheric field. *Journal of Geophysical Research: Space Physics*, *102*(A6), 11,29–11,306. https://doi.org/10.1029/97JA00563

Khurana, K. K. (2001). Influence of solar wind on Jupiter's magnetosphere deduced from currents in the equatorial plane. *Journal of Geophysical Research: Space Physics*, *106*(A11), 25,999–26,016. https://doi.org/10.1029/2000JA000352

Khurana, K. K., & Kivelson, M. G. (1989). On Jovian plasma sheet structure. *Journal of Geophysical Research: Space Physics*, *94*(A9), 11,791–11,803. https://doi.org/10.1029/JA094iA09p11791

Khurana, K. K., Kivelson, M. G., Hand, K. P., & Russell, C. T. (2009). Electromagnetic induction from Europa's ocean and the deep interior. In R. T. Pappalardo, W. B. McKinnon, & K. Khurana (Eds.), *Europa* (pp. 571–586). Tucson: University of Arizona Press.

Khurana, K. K., & Schwarzl, H. K. (2005). Global structure of Jupiter's magnetospheric current sheet. *Journal of Geophysical Research: Space Physics*, *110*(A7). https://doi.org/10.1029/2004JA010757

Kivelson, M. G., Khurana, K. K., Russell, C. T., Walker, R. J., Coleman, P. J., Coroniti, F. V., et al. (1997). Galileo at Jupiter: Changing states of the magnetosphere and first looks at Io and Ganymede. *Advances in Space Research*, *20*(2), 193–204. https://doi.org/10.1016/S0273-1177(97)00533-4

Lanzerotti, L. J., Maclennan, C. G., Krimigis, S. M., Armstrong, T. P., Behannon, K., & Ness, N. F. (1980). Statics of the nightside Jovian plasma sheet. *Geophysical Research Letters*, *7*(10), 817–820. https://doi.org/10.1029/GL007i010p00817

Moore, K. M., Cao, H., Bloxham, J., Stevenson, D. J., Connerney, J. E. P., & Bolton, S. J. (2019). Time variation of Jupiter's internal magnetic

field consistent with zonal wind advection. *Nature Astronomy*, *3*, 730–735. https://doi.org/10.1038/s41550-019-0772-5

Ness, N. F., Acuna, M. H., Lepping, R. P., Burlaga, L. F., Behannon., K. W., & Neubauer, F. M. (1979). Magnetic field studies at Jupiter by Voyager 2: Preliminary results. *Science*, *206*(4421), 966–972. https://doi.org/10.1126/science.206.4421.966

Northrop, T. G., Goertz, C. K., & Thomsen, M. F. (1974). The magnetosphere of Jupiter as observed with Pioneer 10: 2. Nonrigid rotation of the magnetodisc. *Journal of Geophysical Research*, *79*(25), 3579–3582. https://doi.org/10.1029/JA079i025p03579

Ridley, V. A., & Holme, R. (2016). Modeling the Jovian magnetic field and its secular variation using all available magnetic field observations. *Journal of Geophysical Research: Planets*, *121*(3), 309–337. https://doi.org/10.1002/2015JE004951

Smith, E. J., Davis, L., Jr., Jones, D. E., Coleman, P. J., Jr., Colburn, D. S., Dyal, P., et al. (1974). The planetary magnetic field and magnetosphere of Jupiter: Pioneer 10. *Journal of Geophysical Research*, *79*(25), 3501–3513. https://doi.org/10.1029/JA079i025p03501

Stern, D. P. (1970). Euler potentials. *American Journal of Physics*, *38*(4), 494–501. https://doi.org/10.1119/1.1976373

Stern, D. P. (1976). Representation of magnetic fields in space. *Reviews of Geophysics*, *14*(2), 199–214. https://doi.org/10.1029/RG014i002p00199

Van Allen, J. A., Baker, D. N., Randall, B. A., Thomsen, M. F., Sentman, D. D., & Flindt, H. R. (1974). Energetic electrons in the magnetosphere of Jupiter. *Science*, *183*(4122), 309–311. https://doi.org/10.1126/science.183.4122.309

Vogt, M. F., Connerney, J. E. P., DiBraccio, G. A., Wilson, R. J., Thomsen, M. F., Ebert, R. W., et al. (2020). Magnetotail reconnection at Jupiter: A survey of Juno magnetic field observations. *Journal of Geophysical Research: Space Physics*, *125*(3), e2019JA027486. https://doi.org/10.1029/2019JA027486

Yu, Z. J., Leinweber, H. K., & Russell, C. T. (2010). Galileo constraints on the secular variation of the Jovian magnetic field. *Journal of Geophysical Research: Planets*, *115*(E3). https://doi.org/10.1029/2009JE003492